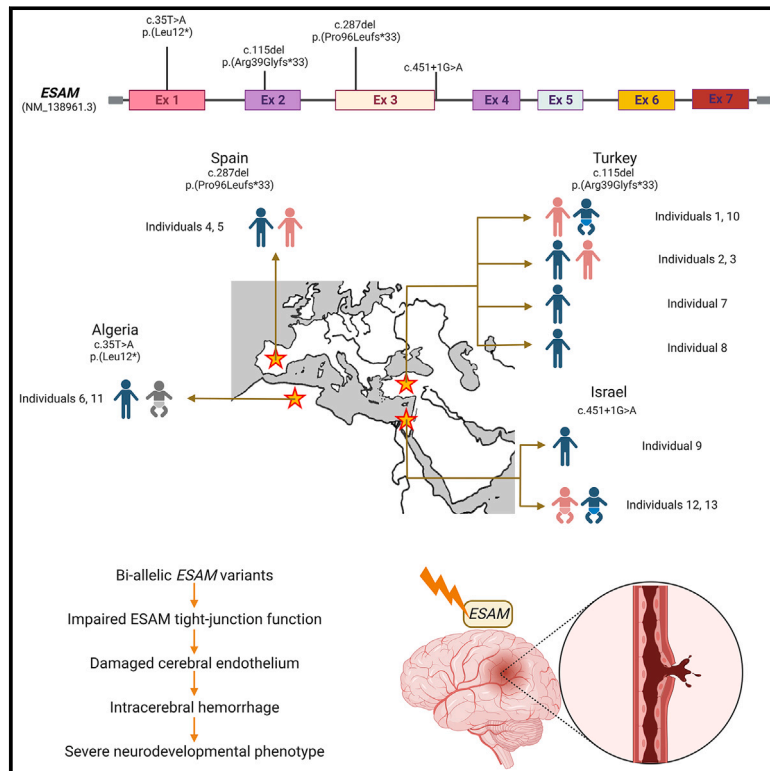


Bi-allelic variants in the *ESAM* tight-junction gene cause a neurodevelopmental disorder associated with fetal intracranial hemorrhage

Graphical abstract



Authors

Mauro Lecca, Davut Pehlivan, Damià Heine Suñer, ..., Ronen Spiegel, James R. Lupski, Edoardo Errichiello

Correspondence

edoardo.errichiello@unipv.it

We identified homozygous loss-of-function variants in *ESAM*, encoding an endothelial cell adhesion molecule, in thirteen individuals (including four fetuses) showing intracerebral hemorrhage in prenatal age and neurodevelopmental disorders. Our findings contribute to expand an emerging group of diseases caused by alterations of tight-junction genes (e.g., *JAM2*, *JAM3*, *OCN*).



Bi-allelic variants in the *ESAM* tight-junction gene cause a neurodevelopmental disorder associated with fetal intracranial hemorrhage

Mauro Lecca,¹ Davut Pehlivan,^{2,3,4} Damià Heine Suñer,^{5,6} Karin Weiss,^{7,8} Thibault Coste,^{9,10} Markus Zweier,¹¹ Yavuz Oktay,^{12,13,14} Nada Danial-Farran,¹⁵ Vittorio Rosti,¹⁶ Maria Paola Bonasoni,¹⁷ Alessandro Malara,^{1,18} Gianluca Contrò,¹⁹ Roberta Zuntini,¹⁹ Marzia Pollazzon,¹⁹ Rosario Pascarella,²⁰ Alberto Neri,²¹ Carlo Fusco,²² Dana Marafi,^{3,23} Tadahiro Mitani,³ Jennifer Ellen Posey,³ Sadik Etkä Bayramoglu,²⁴ Alper Gezdirici,²⁵ Jessica Hernandez-Rodriguez,⁶ Emilia Amengual Cladera,⁶ Elena Miravet,²⁶ Jorge Roldan-Busto,²⁷ María Angeles Ruiz,²⁶ Cristofol Vives Bauzá,²⁸ Liat Ben-Sira,^{29,30} Sabine Sigaudy,³¹ Anaïs Begemann,¹¹ Sheila Unger,³² Serdal Güngör,³³ Semra Hiz,^{13,34} Ece Sonmezler,^{12,13} Yoav Zehavi,^{8,35} Michael Jerdev,³⁶ Alessandra Balduini,^{1,37} Orsetta Zuffardi,¹ Rita Horvath,^{38,39} Hanns Lochmüller,^{40,41,42} Anita Rauch,^{11,43} Livia Garavelli,¹⁹ Elisabeth Tournier-Lasserre,^{9,10} Ronen Spiegel,^{8,35} James R. Lupski,^{3,4,44,45} and Edoardo Errichiello^{1,46,*}

Summary

The blood-brain barrier (BBB) is an essential gatekeeper for the central nervous system and incidence of neurodevelopmental disorders (NDDs) is higher in infants with a history of intracerebral hemorrhage (ICH). We discovered a rare disease trait in thirteen individuals, including four fetuses, from eight unrelated families associated with homozygous loss-of-function variant alleles of *ESAM* which encodes an endothelial cell adhesion molecule. The c.115del (p.Arg39Glyfs*33) variant, identified in six individuals from four independent families of Southeastern Anatolia, severely impaired the *in vitro* tubulogenic process of endothelial colony-forming cells, recapitulating previous evidence in null mice, and caused lack of *ESAM* expression in the capillary endothelial cells of damaged brain. Affected individuals with bi-allelic *ESAM* variants showed profound global developmental delay/unspecified intellectual disability, epilepsy, absent or severely delayed speech, varying degrees of spasticity, ventriculomegaly, and ICH/cerebral calcifications, the latter being also observed in the fetuses. Phenotypic traits observed in individuals with bi-allelic *ESAM* variants overlap very closely with other known conditions characterized by endothelial dysfunction due to mutation of genes encoding tight junction molecules. Our findings emphasize the role of brain endothelial dysfunction in NDDs and contribute to the expansion of an emerging group of diseases that we propose to rename as “tightjunctionopathies.”

¹Department of Molecular Medicine, University of Pavia, Pavia, Italy; ²Section of Pediatric Neurology and Developmental Neuroscience, Department of Pediatrics, Baylor College of Medicine, Houston, TX, USA; ³Department of Molecular and Human Genetics, Baylor College of Medicine, Houston, TX, USA; ⁴Texas Children's Hospital, Houston, TX, USA; ⁵Molecular Diagnostics and Clinical Genetics Unit, Hospital Universitari Son Espases, Palma, Illes Balears, Spain; ⁶Genomics of Health, Institute of Health Research of the Balearic Islands, Palma, Illes Balears, Spain; ⁷Genetics Institute, Rambam Health Care Campus, Haifa, Israel; ⁸The Ruth and Bruce Rappaport Faculty of Medicine, Technion-Israel Institute of Technology, Haifa, Israel; ⁹AP-HP, Service de Génétique Moléculaire Neurovasculaire, Hôpital Saint-Louis, Paris, France; ¹⁰Université de Paris, INSERM UMR-1141 Neurodiderot, Paris, France; ¹¹Institute of Medical Genetics, University of Zurich, Schlieren-Zurich, Switzerland; ¹²Izmir Biomedicine and Genome Center, Dokuz Eylul University Health Campus, Izmir 35340, Turkey; ¹³Izmir International Biomedicine and Genome Institute, Dokuz Eylul University, Izmir 35340, Turkey; ¹⁴Department of Medical Biology, School of Medicine, Dokuz Eylul University, Izmir 35340, Turkey; ¹⁵The Genetic Institute, Emek Medical Center, Afula, Israel; ¹⁶Center for the Study of Myelofibrosis, Laboratory of Biochemistry, Biotechnology and Advanced Diagnosis, IRCCS Policlinico San Matteo Foundation, Pavia, Italy; ¹⁷Pathology Unit, Azienda USL-IRCCS di Reggio Emilia, Reggio Emilia, Italy; ¹⁸Laboratory of Biochemistry-Biotechnology and Advanced Diagnostics, IRCCS Policlinico San Matteo Foundation, Pavia, Italy; ¹⁹Medical Genetics Unit, Azienda USL-IRCCS di Reggio Emilia, Reggio Emilia, Italy; ²⁰Neuroradiology Unit, Azienda USL-IRCCS di Reggio Emilia, Reggio Emilia, Italy; ²¹Ophthalmology Unit, Azienda USL-IRCCS di Reggio Emilia, Reggio Emilia, Italy; ²²Child Neurology and Psychiatry Unit, Azienda USL-IRCCS di Reggio Emilia, Reggio Emilia, Italy; ²³Department of Pediatrics, Faculty of Medicine, Kuwait University, P.O. Box 24923, Safat 13110, Kuwait; ²⁴Tertiary ROP Center, Health Science University Kanuni Sultan Suleyman Training and Research Hospital, Istanbul 34303, Turkey; ²⁵Department of Medical Genetics, Basaksehir Cam and Sakura City Hospital, Istanbul 34480, Turkey; ²⁶Metabolic Pathologies and Pediatric Neurology Unit, Pediatric Service, Hospital Universitari Son Espases, Palma, Illes Balears, Spain; ²⁷Pediatric Radiology Unit, Radiology Service, Hospital Universitari Son Espases, Palma, Illes Balears, Spain; ²⁸Neurobiology, Institute of Health Research of the Balearic Islands, Palma, Illes Balears, Spain; ²⁹Department of Radiology, Division of Pediatric Radiology, Dana Children's Hospital, Tel Aviv Sourasky Medical Center, Tel Aviv University, Tel Aviv, Israel; ³⁰Sackler School of Medicine, Tel Aviv University, Tel-Aviv, Israel; ³¹AP-HM, Service de Génétique, Hôpital de la Timone, Marseille, France; ³²Medical Genetics Service, CHUV, University of Lausanne, Lausanne, Switzerland; ³³Inonu University, Faculty of Medicine, Turgut Ozal Research Center, Department of Pediatric Neurology, Malatya, Turkey; ³⁴Department of Pediatric Neurology, School of Medicine, Dokuz Eylul University, Izmir 35340, Turkey; ³⁵Department of Pediatrics B, Emek Medical Center, Afula, Israel; ³⁶Poriya Medical Center and the Azrieli Faculty of Medicine, Bar-Ilan University, Ramat-Gan, Israel; ³⁷Department of Biomedical Engineering, Tufts University, Medford, MA, USA; ³⁸Department of Clinical Neurosciences, School of Clinical Medicine, University of Cambridge, Cambridge Biomedical Campus, Cambridge CB2 0PY, UK; ³⁹Department of Clinical Neurosciences, John Van Geest Centre for Brain Repair, School of Clinical Medicine, University of Cambridge, Cambridge CB2 0PY, UK; ⁴⁰Children's Hospital of Eastern Ontario Research Institute, University of Ottawa, Ottawa, ON K1H 8L1, Canada; ⁴¹Brain and Mind Research Institute, University of Ottawa, Ottawa ON K1H 8L1, Canada; ⁴²Division of Neurology, Department of Medicine, The Ottawa Hospital, Ottawa, ON K1H 8L1, Canada; ⁴³University Children's Hospital Zurich, University of Zurich, Zurich, Switzerland; ⁴⁴Department of Pediatrics, Baylor College of Medicine, Houston, TX, USA; ⁴⁵Human Genome Sequencing Center, Baylor College of Medicine, Houston, TX, USA; ⁴⁶Neurogenetics Research Center, IRCCS Mondino Foundation, Pavia, Italy

*Correspondence: edoardo.errichiello@unipv.it

<https://doi.org/10.1016/j.ajhg.2023.03.005>

© 2023 American Society of Human Genetics.



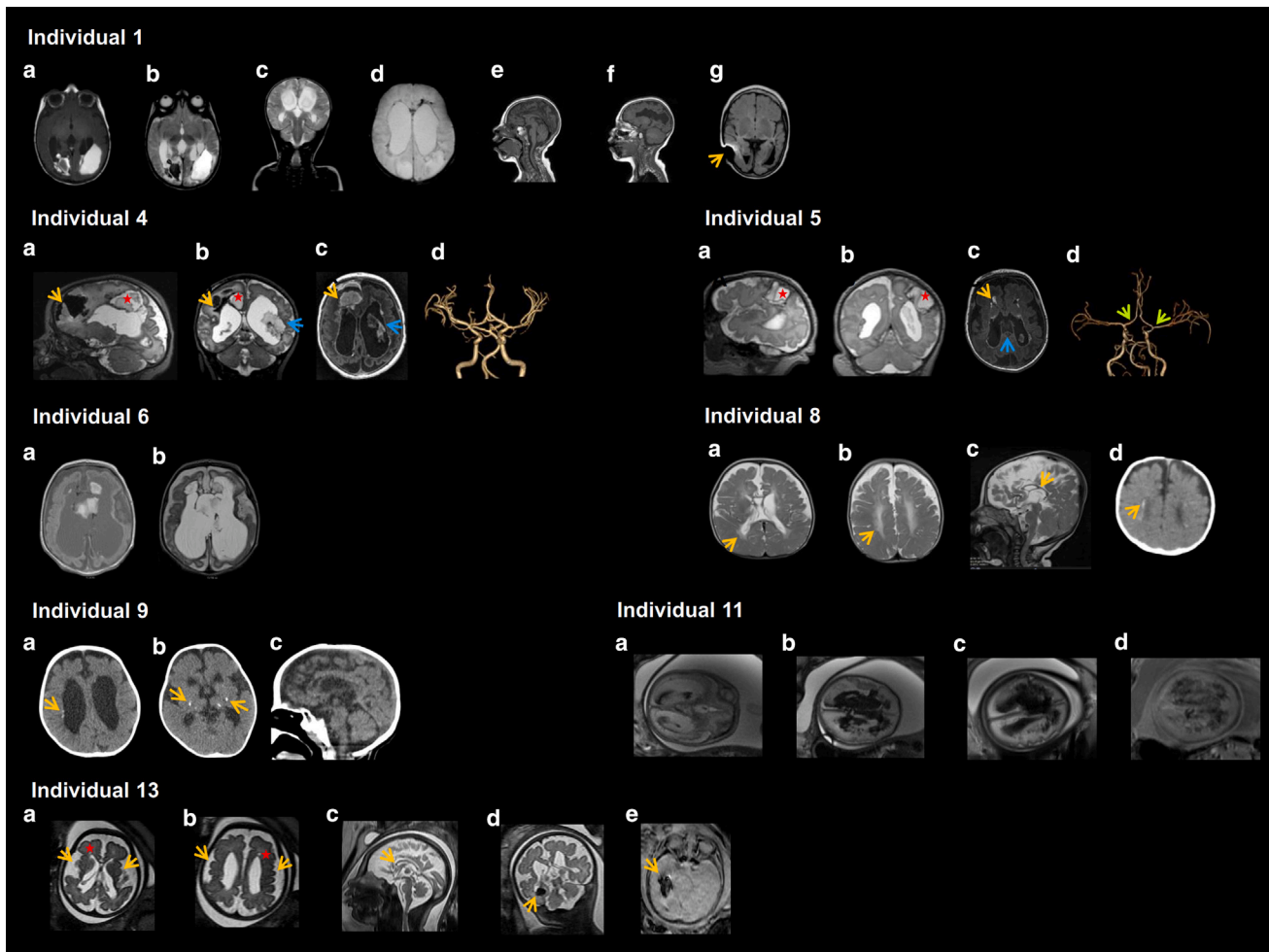


Figure 1. Neuroimaging abnormalities in individuals with homozygous *ESAM* variants

Individual 1: T1-weighted (a and b) images showing various parenchymal hemorrhagic area in different evolution phases, located at the parietal-occipital area. T2-weighted and multi-echo gradient-recalled echo (GRE) T2-weighted images (c and d) showing blood occupying the ventricular spaces (hemoventricle). T1-weighted MRI (e and f) and FLAIR sequences (g) highlight a dysmorphic corpus callosum (e) and poromalacic evolution of the hemorrhagic areas with ventricular dilatation (f and g) and diffuse subependymal microhemorrhage foci. The orange arrow in (g) indicates ventricular derivation.

Individual 4: MRI images at 2 days after birth: 3DT2 sagittal (a), 3DT2 coronal MPR (b), 3DT1 axial (c), 3D TOF (d). Bilateral grade III germinal matrix - intraventricular hemorrhage (blue arrows) with supratentorial posthemorrhagic hydrocephalus. Bilateral parenchymal hematomas with associated subpial hemorrhages (orange arrows) at different stages and parietal encephalomalacia secondary to prior bleeding with residual clot inside (red stars). No evident vascular anomalies in MRI angiography (3D TOF sequence) were found.

Individual 5 (sibling of individual 4): MRI images at 7 days after birth: 3DT2 sagittal (a), 3DT2 coronal MPR (b), 3DT1 axial (c), 3D TOF (d). Microcephaly with simplified gyral pattern and severe hypoplastic corpus callosum (blue arrow). Left parietal subcortical white matter hematoma with subpial hemorrhage (red stars) and encephalomalacia. Right frontal (orange arrow) and multiple bilateral periventricular hemorrhages. MRI angiography (3D TOF sequence) shows slight narrowing of the proximal anterior and middle cerebral arteries (green arrows).

Individual 6: MRI images at 5 days old. T1- (a) and T2- (b) weighted images showing massive dilatation of lateral ventricles with global cerebral parenchymal destruction. Diffuse meningeal and intraventricular hemorrhage with intraventricular clotting. Focal destruction of the septum pellucidum.

Individual 8: axial T2-weighted images showed hyperintensity and volume loss in the bilateral periventricular white matter, frontotemporal atrophy, dilatation in the lateral ventricles (a and b) and hypoplasia of the corpus callosum (c) (orange arrows). Bilateral periventricular calcifications were observed on cranial CT (d), as indicated by the arrow.

Individual 9: Head CT (axial) showing bilateral subependymal (a) and basal ganglia/thalamus calcifications (b) (orange arrows), suggestive of a previous bleeding. Dilatation of the lateral ventricles and their straight shape suggest agenesis of the corpus callosum, as confirmed in the sagittal multiplanar reformation (c).

Individual 11: Axial T2-weighted true fast sequence (a and b), axial T2 HASTE sequence (c), and axial T1-weighted sequence (d). The fetal brain MRI shows hydrocephalus, intraventricular hemorrhage, diffuse intraparenchymal, and periventricular hemorrhages with calcifications (hypointense signals on T1-weighted images).

Individual 13: Brain MRI at 37 weeks of gestation. Axial T2 (a and b) showing severe irregular ventriculomegaly with increased extra-axial spaces and significant decrease in gray and white matter volume. Orange arrows indicate an abnormal Sylvian fissure development in

(legend continued on next page)

Neurodevelopmental disorders (NDDs) are a large group of disabilities involving impairment of the brain and neurocognitive development affecting >3% of children worldwide.¹ NDDs include a broad spectrum of phenotypes such as intellectual disability/developmental delay (ID/DD), autism spectrum disorders (ASD), attention-deficit/hyperactivity disorder (ADHD), epilepsy, cerebral palsy, and language impairment. Comorbidity of two or more of these conditions is frequently observed.² Furthermore, neuroimaging findings, such as corpus callosum and white matter anomalies, may suggest a specific etiology for NDD.³ At least 30% of NDDs are thought to have a genetic basis, and a plethora of genes and molecular alterations have been identified, underlying wide clinical and genetic heterogeneity, overlapping phenotypes, and gene pleiotropy, which together make molecular diagnosis a challenging task.^{4,5} The implementation of next-generation sequencing (NGS) technologies, especially exome sequencing (ES), which has been proposed as a first-tier test in the diagnostic algorithm of all NDDs followed by array-CGH when necessary, has dramatically increased the percentage of NDD-affected individuals who receive a molecular diagnosis.⁶ Furthermore, diagnostic rates reported in recent studies and meta-analyses are 30%–40% or higher when trio analysis is performed and when NDD-affected individuals eligible for diagnostic ES are prioritized before testing based on their phenotypic presentation.^{7–13}

Prenatal/perinatal brain damage due to intracranial/intraventricular hemorrhage (ICH/IVH) is one of the leading causes of lifelong disability, including cerebral palsy, epilepsy, sensory impairment, and cognitive deficit.^{14–18} The blood-brain barrier (BBB), whose integrity is maintained by junctional adhesion molecules (JAMs), is considered the core structure of the neurovascular unit (NVU) and plays a critical role in maintaining central nervous system homeostasis. Tight junctions (TJs) are an essential BBB component and bi-allelic variants in the tight-junction genes *JAM2/3* (junctional adhesion molecule 2/3 [MIM: 606870 and 606871]) and *OCN* (occludin [MIM: 602876]) have been implicated in individuals with compromised BBB permeability. These subjects typically show a combination of brain hemorrhage and calcification together with movement disorders and cognitive and neurobehavioral manifestations.^{19–24}

In this study, we identified bi-allelic variants in *ESAM* (endothelial cell adhesion molecule [MIM: 614281]), a gene not previously associated with a rare disease trait in humans, which encodes a TJ protein related to JAM proteins involved in the formation and maintenance of the BBB. Genotypic (ES) and clinical phenotypic data from individuals with *ESAM* variants were recruited

through GeneMatcher²⁵ and our international collaborative network. All individuals were carefully evaluated by a multidisciplinary team of pediatric neurologists/neuroophthalmologists/neuroradiologists and clinical geneticists of their respective referral center. We collected clinical information related to neurodevelopment, growth parameters, dysmorphology, neurological, ocular, and vascular manifestations, plus behavior and neuroimaging. No formal intelligence testing was possible in individuals over the age of 5 years because of the severe global developmental delay, including complete lack of language and motor skills. Written human subject research informed consent for genetic analysis and publication of the clinical information, including relevant clinical pictures, was obtained from the parents or legal guardians of each research subject according to the Declaration of Helsinki and Institutional Review Boards of participating research centers.

The age of affected individuals included in the study, 8 males and 4 females (sex was unknown in a 32-week-old fetus), ranged from 31 weeks of gestation to 13 years. Onset of symptoms occurred in the antenatal/neonatal period. Global developmental delay/unspecified intellectual disability (GDD/UID), absent or severely delayed speech, epilepsy, spasticity (mainly consisting of spastic tetraparesis), hypotonia (which frequently occurred neonatally), and dilation of lateral ventricles were observed in all nine live-born children, the latter being also noted in the four fetuses examined in the study (Table S1), while variable microcephaly was reported in four out of nine children (mean OFC Z score: -3.35 ; range: -2.1 to -5.7). Following dilation of lateral ventricles, thinning of the corpus callosum, hydrocephalus, and focal white matter lesions were the most frequently observed neuroimaging abnormalities (eight, seven, and five individuals, respectively) (Figure 1). Notably, hydrocephalus was a feature also observed in all fetuses as well as in a previously reported individual carrying an *ESAM* homozygous nonsense variant (Table S1).²⁶ Intracranial hemorrhages (ICH) or suspected cerebral microangiopathy, frequently associated with cerebral calcifications (Figure 1), were reported in all individuals, including the four fetuses. Other vascular anomalies were represented by retinal hemorrhage (four individuals)—due to increased tortuosity of retinal vasculature (Figures S1 and S2)—and renal medullary hemorrhage (in a 31-week stillbirth). Dysmorphic facial features were noted in most individuals, mainly consisting of bitemporal narrowing (6/9), highly arched eyebrow and bulbous nasal tip, which were detected with the same frequency (5/9), followed by presence of long eyelashes (4/9), abnormal vermilion (4/9), high narrow palate (3/9), wide nasal bridge (3/9),

(a) and an asymmetric gyral pattern suggestive of dysgyria/polymicrogyria in (b). Small periventricular cysts are indicated by red stars. Sagittal T2 (c) highlighting corpus callosum dysgenesis with absence of rostrum (arrow). Coronal T2 (d): hypointense lesions in the temporal parenchyma (indicated by the arrow) protruding into the temporal horn of the right ventricle. GRE T2 sequences (e) demonstrate susceptibility artifacts consistent with brain calcification (arrow).

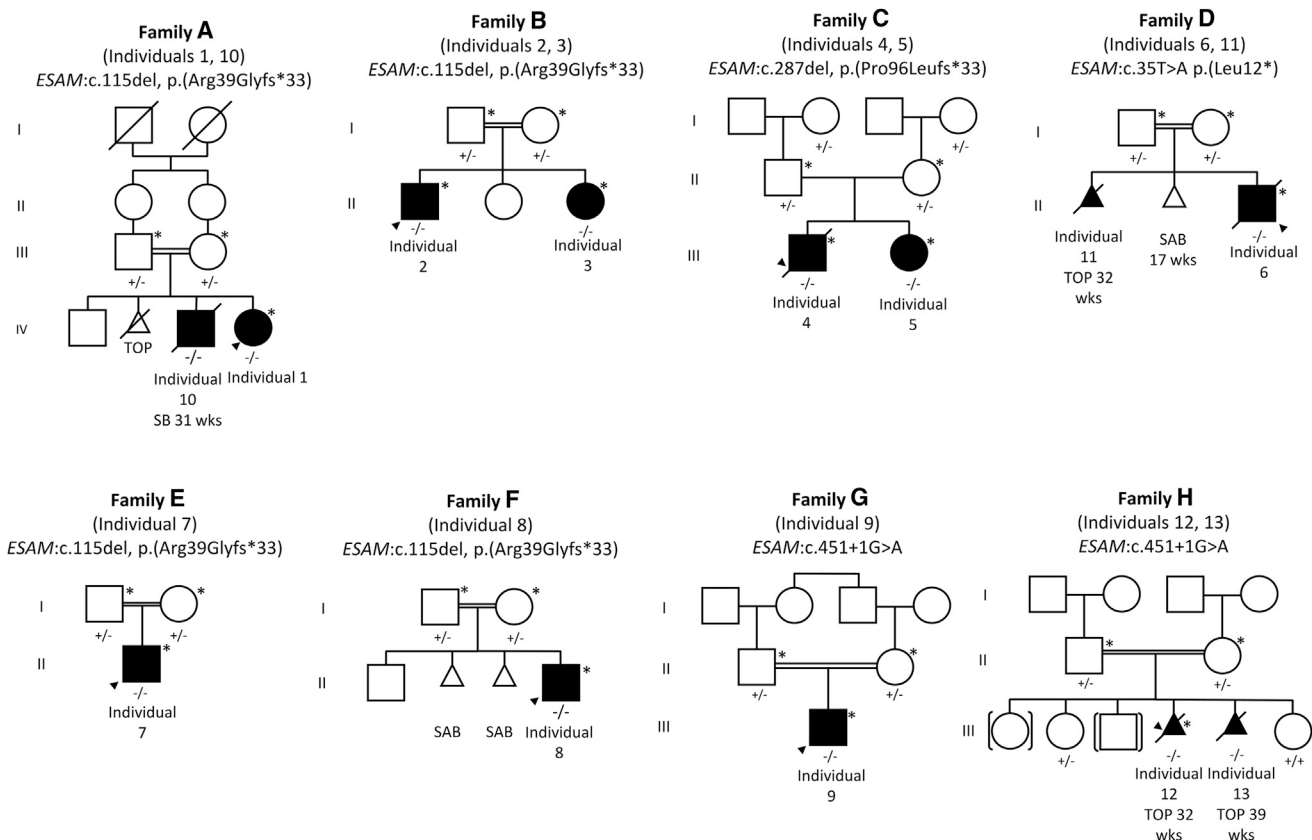


Figure 2. Family pedigrees and genetic findings

Bi-allelic *ESAM* variants are shown in thirteen affected individuals, including four fetuses, from eight unrelated families. The c.115del (p.Arg39Glyfs*33) frameshift variant was identified in six individuals from families A, B, E, and F, originating from the same geographic area in Turkey (southeastern Anatolia). The c.287del (p.Pro96Leufs*33) frameshift variant was detected in two affected siblings from a family of Spain (family C). The c.35T>A (p.Leu12*) nonsense variant was identified in a family of Algerian descent (family D). The c.451+1G>A splice site variant was identified in two independent families of Arab Bedouin descent (families G and H). +/+, +/-, and -/- represents homozygosity for the wild-type allele, heterozygosity, and homozygosity for the mutant allele, respectively. An asterisk beneath an individual indicates that ES was performed. Arrowheads indicate the probands. TOP, termination of pregnancy; SB, stillbirth; SAB, spontaneous abortion; wks, weeks of gestation.

upslanted palpebral fissures (3/9), and microretrognathia (2/9), the latter being also present in a fetus (Table S1 and supplemental note).

ES identified homozygous *ESAM* loss-of-function (LoF) variant alleles in all affected individuals belonging to eight independent families (from A to H) (Figure 2 and supplemental note). The same frameshift variant in exon 2, c.115del (p.Arg39Glyfs*33), was detected in six individuals from four unrelated families, including a 31-week stillbirth (individuals 1, 2, 3, 7, 8, and 10). Individuals 4 and 5 are affected siblings carrying the c.287del (p.Pro96Leufs*33) frameshift variant in exon 3. Individual 6 harbored a nonsense variant within the first gene exon, c.35T>A (p.Leu12*). Although archival autopsy material was not available for his affected sibling (individual 11), a fetus of 32 weeks, it is highly likely that the same variant was present based on strict phenotypic comparison. Individuals 9, 12, and 13 carried the same homozygous splice variant in intron 3 (c.451+1G>A) predicted to cause loss of donor splice site by multiple *in silico* tools (e.g., HSF, MaxEntScan, SpliceAI, CADD-Splice). In all probands no other poten-

tially relevant variants were identified either in known genes associated with neurological and vascular conditions/phenotypes, according to PanelApp, HPO, and GTR, or by filtering the variants for coherent inheritance patterns.

Interestingly, all individuals harboring the c.115del variant originated from the same geographic region in Turkey (southeastern Anatolia), suggesting a founder effect. The variant was not reported in the SHGP (Saudi Human Genome Program) database, the largest genome repository in the Middle East,^{27,28} nor in the Iranome database,²⁹ the GME (Greater Middle East) Variome Project,³⁰ or the Turkish Variome (TRV) database.³¹ Similarly, the c.451+1G>A variant was detected in three individuals from two independent families with the same ethnic origin (Arab Bedouin) and was also absent in the aforementioned databases.

All the variants were classified as likely pathogenic according to the ACMG/AMP criteria (PVS1+PM2) and were predicted to trigger nonsense-mediated mRNA decay (NMD). In all cases, *ESAM* was embedded in ROH/AOH

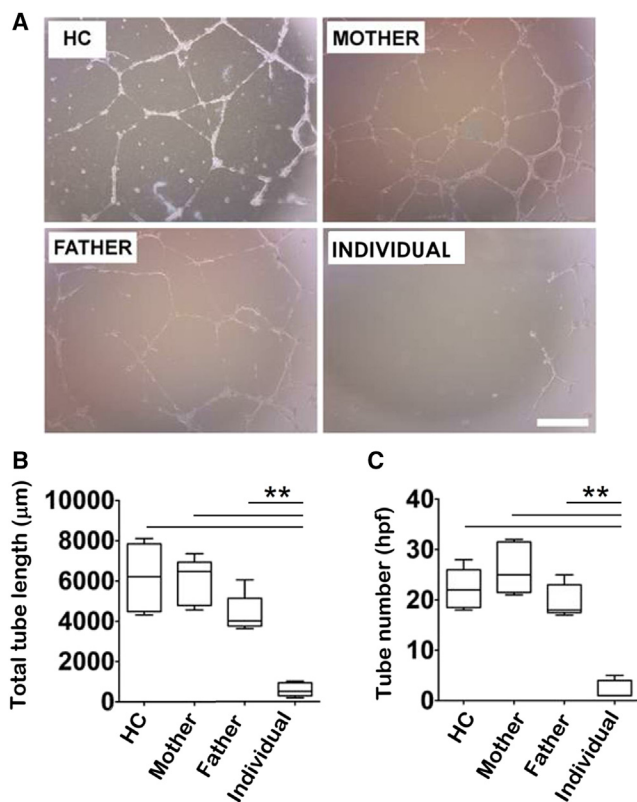


Figure 3. *In vitro* matrigel tubulogenesis assay

(A) Endothelial colony-forming cells (ECFCs) isolated from individual 1 showed significantly decreased tubulogenesis compared to the ECFCs obtained from a healthy control (HC) and parents of individual 1.

(B and C) Quantification of tubulogenesis was performed considering the number of branch points (B) and the tube length (C). Data shown (\pm SD) are from 3 independent experiments. ****** $p < 0.01$. Scale bar: 200 μ m. More technical details are provided in the [supplemental note](#).

(runs of homozygosity/absence of heterozygosity) stretches spanning from 1.8 to 13.85 Mb in size, consistent with shared ancestry and/or recent consanguinity. Details of the variants are publicly available in the ClinVar database (<https://www.ncbi.nlm.nih.gov/clinvar/>) with the following accession numbers: SCV002818296 (c.115del), SCV002818297 (c.287del), SCV002818299 (c.35T>A), and SCV002818300 (c.451+1G>A). The predicted 3D structures of the mutant protein products are shown in [Figure S3](#). The crucial immunoglobulin-like (Ig) domains (aa 30–150 and 157–239) and the helical transmembrane domain (aa 247–279) were abolished, whereas the putative motifs predicted by AlphaFold (<https://alphafold.ebi.ac.uk/>), which are absent in the wild-type protein, did not match with any known protein signature explored through different databases and bioinformatic tools (e.g., Motif Scan, ScanProsite, BlastP).

Considering the crucial role of ESAM in angiogenesis, endothelial permeability, and leukocyte transmigration^{32,33} as well as its enriched expression in the endothelium (GTEx, BioGPS, HPA) and the peculiar vascular alter-

tations observed in the identified individuals harboring *ESAM* variants (especially of the brain), we assessed the capability of endothelial progenitors (endothelial colony-forming cells [ECFCs]) to form capillary-like structures *in vitro*. Compared to an age- and sex-matched control sample, ECFCs of individual 1 showed dramatic phenotypical changes of proliferation, migration, and tubulogenesis ([Figure 3A](#)) in terms of both number of branch points and tube length ([Figures 3B and 3C](#)), which were almost completely abrogated. On the other hand, the ECFCs isolated from her healthy heterozygous parents showed comparable values to the control sample.

The fetal brain of individual 10, carrying the c.115del (p.Arg39Glyfs*33) homozygous frameshift variant, showed lack of *ESAM* staining in the capillary endothelial cells ([Figure 4A](#)), which is consistent with the LoF effect of the c.115del bi-allelic variant. On the other hand, intense expression of *ESAM* was observed in the cerebral endothelium of an age- and sex-matched control sample, where it was abundantly localized in the plasma membrane of endotheliocytes ([Figure 4B](#)). The immunohistochemical findings are in agreement with the results of reverse transcription polymerase chain reaction (RT-PCR) performed on ECFCs of individual 1, showing no detectable *ESAM* expression ([Figure S4](#)), as well as with the *in silico* NMD predictions and the 3D-modeling, which overall indicate a lack of functional protein. Furthermore, microscopic and histochemical analysis revealed periventricular leukomalacia ([Figure 4C](#)) and brain calcification with abundant presence of so-called "ferruginated" neurons, implying mineralization of neurons as a consequence of hypoxic-ischemic damage ([Figure 4D](#)).

In this study, we describe a severe neurodevelopmental rare disease trait caused by homozygous LoF variants of *ESAM* in thirteen individuals, including four fetuses, from eight unrelated families. Global developmental delay/unspecified intellectual disability (GDD/UID) with absent or severely delayed speech, epilepsy, varying degrees of spasticity, ventriculomegaly, and intracranial hemorrhage constitute the cardinal clinical features of the *ESAM*-related phenotype, being observed in all live-born individuals. Other notable clinical signs were thin corpus callosum and variable microcephaly. Among the clinical features, intracranial hemorrhage, together with hydrocephalus and cerebral calcifications, represented the first observable prenatal anomalies that prompted further genetic investigations and, thus, is hypothesized as the etiological trigger of downstream neurodevelopmental defects. In addition to the frank neurological manifestations, *ESAM* alterations also appear to cause a well-defined spectrum of ophthalmological signs, particularly retinal ischemia and abnormal retinal vascular morphology.

ESAM encodes an endothelial cell-selective adhesion molecule, a member of the immunoglobulin receptor family, which mediates homophilic interactions between endothelial cells. Previous studies demonstrated that

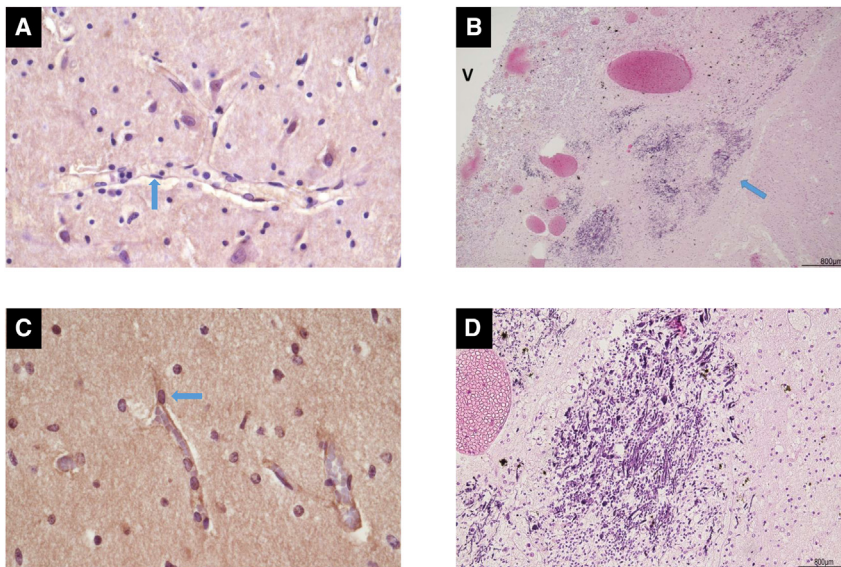


Figure 4. ESAM immunohistochemistry and hematoxylin and eosin staining in the damaged brain tissue (white matter) of individual 10

(A and B) A capillary with ESAM-negative endothelial cells in the proband (A) compared to a control sample (B), as indicated by the blue arrows. Magnification: 40 HPF.

(C) Periventricular leukomalacia in individual 10: the white matter close to the lateral ventricle (V) shows multiple areas of calcification (blue arrow). Hematoxylin and eosin staining, magnification 4 HPF.

(D) Calcified areas showing elongated sticks and round bodies as a result of encrusted ("ferruginated") neurons and their axons with mineral salts. Hematoxylin and eosin staining, magnification 20 HPF. More technical details are provided in the [supplemental note](#).

ESAM expression is primarily restricted to embryonic and adult vasculature, where it regulates endothelial permeability and neutrophil extravasation.^{33–35} Mouse model experiments showed that *ESAM* regulates albumin extravasation at the glomeruli and plays a role in the initiation of diabetic nephropathy.³⁶ A recent proteomic study of individuals affected by diabetic kidney disease confirmed *ESAM* as a candidate circulating biomarker to predict the risk of progression to kidney failure.³⁷ In this regard, we did not observe renal dysfunction in our pediatric subjects, although later manifestations cannot be completely ruled out and careful follow-up in the next years would be indicated. Interestingly, a proteomic analysis revealed that *ESAM* interacts with endoglin,³⁸ encoded by *ENG*, whose mutation causes hereditary hemorrhagic telangiectasia (HHT [MIM: 187300]), a condition that includes ICH as a clinical feature.

In a previous study, a *de novo* heterozygous frame-shift variant in *ESAM* exon 4, c.543_546dup (p.Val1183Argfs*48), was reported in a 23-year-old male individual affected by schizophrenia and developmental delay.³⁹ Therefore, it could be hypothesized that monoallelic LoF variants in *ESAM* may at most contribute (possibly together with other factors) to mild neurological phenotypes, in contrast to the severe phenotype we observed in all our homozygous probands. Nevertheless, we did not observe overt neuropsychiatric features in any of our probands' heterozygous parents nor in other carrier family members. This finding is in line with the gene constraint metrics (pLI: 0.20; LOEUF: 0.59; sHet: 0.05; %HI: 63.38) and the presence of an ~34 kb deletion encompassing *ESAM* in the DGV (Database of Genomic Variants) repository (nsv556487), indicating that *ESAM* is quite tolerant to haploinsufficiency, as it is for triplosensitivity (pTripto: 0.28).⁴⁰ Altogether, it is at most possible to speculate that heterozygous LoF variants may represent a susceptibility factor characterized by incomplete penetrance,

and, in any case, further studies are needed to better address this point.

Our *in vitro* tubulogenesis assays recapitulated findings in null mice (*Esam*^{-/-}) where a decrease of tube formation and vascular density was documented, although without overt morphological defects of the vasculature.³² On the contrary, we observed a high frequency of vascular manifestations (intracranial hemorrhage, cerebral calcifications, focal white matter lesions, hydrocephalus, and dilation of lateral ventricles), in agreement with the critical role of *ESAM* in endothelial homeostasis. The fact that both null mice and human subjects carrying homozygous LoF variants in *ESAM* show a non-lethal (although extremely severe) phenotype could potentially be explained considering the redundant functional role of *ESAM* in physiological angiogenesis and the presence of other endothelial adhesion molecules which may compensate for its dysfunction.

It is noteworthy that the phenotype associated with bi-allelic variants of *ESAM* overlaps very closely with other known conditions characterized by endothelial dysfunction due to mutation of genes encoding tight junction molecules, namely *JAM2*, *JAM3*, and *OCN*. Bi-allelic LoF variants of *JAM2* are associated with idiopathic basal ganglia calcification (IBGC8 [MIM: 618824]), a condition commonly characterized by intracerebral calcifications, cognitive decline, learning difficulties, seizures, slurred speech, movement disorders, and psychiatric symptoms.^{19,20} Homozygous LoF variants in *JAM3* have been identified in individuals with multifocal intraparenchymal hemorrhage and subependymal calcification as cardinal features (HDBSCC [MIM: 613730]), accompanied by reduced white matter volume, porencephaly, and massive cystic degeneration resulting in enlarged ventricles.^{21,22} In most of the cases, this condition is extremely severe, with death occurring in the first few weeks of life, while alive individuals develop profound developmental

Table 1. Phenotypic comparison of individuals with bi-allelic variants in *JAM2*, *JAM3*, *OCLN*, and *ESAM*

Clinical features	<i>JAM2</i>	<i>JAM3</i>	<i>OCLN</i>	<i>ESAM</i>
Head and neck				
Microcephaly	no	yes	yes	yes
Cataracts	no	yes	yes (rare)	no
Facial dysmorphisms	no	no	yes: long philtrum, microretrognathia, low-set ears, anteverted nares, high arched palate	yes: bitemporal narrowing, highly arched eyebrow, bulbous nasal tip, long eyelashes, high narrow palate, wide nasal bridge, upslanted palpebral fissures, microretrognathia, anteverted nares
Neurologic				
Developmental delay	yes	yes (severe)	yes (severe)	yes (severe)
Seizures	yes (rare)	yes	yes	yes
Spasticity	yes	yes	yes	yes
Hypotonia	no	yes	yes	yes
Neuroimaging findings				
Intracranial calcifications	yes	yes	yes	yes
Intracranial hemorrhage	no	yes	no	yes
Ventriculomegaly	no	yes	yes	yes
Corpus callosum anomalies	no	yes	yes	yes
Abdomen				
Hepatomegaly	no	yes	yes	no
Genitourinary				
Renal anomalies	no	yes (rare)	yes (rare)	yes (rare) (renal medullary hemorrhage)
Disease onset	adulthood	neonatal	neonatal	antenatal/neonatal

delay, microcephaly, generalized spasticity, and seizures, as we observed in our cohort of affected individuals. Finally, bi-allelic LoF variants affecting a tight junction protein, occludin, have been reported in individuals showing profound developmental delay, early-onset seizures, microcephaly, ventriculomegaly, spasticity, polymicrogyria, loss of white matter, and intracranial calcifications, referred to as pseudo-TORCH syndrome 1 (PTORCH1 [MIM: 251290]).^{23,24} Overall, neurological manifestations (namely DD, seizures, spasticity, and hypotonia) and intracranial calcifications represent the cardinal clinical features shared among these conditions, which we also observed in *ESAM*-affected individuals, whereas ICH seems specifically restricted to *JAM3*- and *ESAM*-related phenotypes (Table 1). Furthermore, individuals with pathogenic variants in *COL4A1*, encoding type IV collagen alpha-1 chain protein (a vascular basement membrane protein highly expressed in brain vessels), show intracerebral hemorrhage with calcifications, porencephaly, cystic brain lesions, hydrocephalus, seizures, and retinal arterial tortuosity.^{41–45} In aggregate these data suggest that defective cell adhesion and solute flux through the paracellular spaces in the neurovascular unit (NVU) is a key pathomechanism of brain calcification and hemorrhage in this group of disorders, which we here propose to rename as “tightjunctionopathies.”

Prenatal ICH is a strong risk factor for perinatal mortality and adverse neurodevelopmental outcome. In a recent systematic review, cerebral palsy (CP) was observed at postnatal follow-up in 32% of fetuses with prenatal diagnosis of ICH, in most cases accompanied by severe neurodevelopmental delay.¹⁸ Accordingly, we observed varying degrees of spasticity (mainly consisting of spastic tetraparesis) in all children with bi-allelic *ESAM* variants, together with GDD/UID and other neurological manifestations. Genetic testing is rarely considered in the diagnostic workup of CP individuals, although a recent systematic review and meta-analysis reported non-negligible diagnostic yields of ES and CMA (23% and 5%, respectively).⁴⁶ Our findings add a piece of knowledge to the genetic causes of CP conferring vulnerability to brain injury during prenatal life and causing long-term neurodevelopmental complications.

In summary, our study reveals a rare Mendelian condition associated with bi-allelic *ESAM* variants and emphasizes the increasingly emerging role of brain endothelial dysfunction in neurodevelopmental disorders. In fact, the interplay between vascular and neuronal systems is critical for the normal growth and function of neurons, considering that brain development relies heavily on proper cerebrovascular maturation forming a complex system of multidirectional communication

known as the “neuro-glial-vascular” unit.^{47–50} Therefore, it is conceivable that alterations in cerebrovascular processes during early development may have long-lasting neurodevelopmental consequences, including non-malformative conditions. In fact, endothelial dysfunction leading to impaired cerebral angiogenesis has been documented in a mouse model hemizygous for the ASD-related 16p11.2 deletion, pointing to a potential role for endothelial impairment in ASD pathogenesis.⁵¹ In this regard, a previous ASD postmortem brain study suggested an impairment in cerebral angiogenesis,⁵² whereas a functional imaging study proposed a possible link between ASD and altered cerebral blood flow.⁵³ Altogether, these data also open a new perspective on potential treatment options for mitigating endothelial cell dysfunction in neurodevelopmental conditions due to altered BBB function.

Data and code availability

The published article includes all datasets generated or analyzed during this study. In particular, details of the variants are publicly available in the ClinVar database (<https://www.ncbi.nlm.nih.gov/clinvar/>) with the following accession numbers: SCV002818296 (c.115del), SCV002818297 (c.287del), SCV002818299 (c.35T>A), and SCV002818300 (c.451+1G>A).

Supplemental information

Supplemental information can be found online at <https://doi.org/10.1016/j.ajhg.2023.03.005>.

Acknowledgments

The authors thank all probands and families for their participation in this study. More details are provided in the [supplemental note](#).

Author contributions

M.L.: Data curation, Investigation, Validation, Visualization; D.P., D.H.S., K.W., T.C., M.Z., Y.O., N.D.-F.: Funding acquisition, Investigation, Validation, Supervision; V.R., M.P.B., A.M., R.Z., D.M., T.M., J.E.P., J.H.-R., E.A.C., E.M., C.V.B., E.S.: Investigation; G.C., M.P., R.P., A.N., C.F., S.E.B., A.G., J.R.-B., M.A.R., L.B.S., S.S., A. Begemann, S.U., S.G., S.H., Y.Z., M.J.: Resources; A. Balduini, O.Z., R.H., H.L., A.R., L.G., E.T.-L., R.S., J.R.L.: Supervision, Funding acquisition, Writing – review & editing; E.E.: Conceptualization, Data curation, Formal Analysis, Funding acquisition, Investigation, Project administration, Supervision, Validation, Visualization, Writing – original draft, Writing – review & editing

Declaration of interests

J.R.L. has stock ownership in 23andMe and is a paid consultant for the Regeneron Genetics Center.

Received: January 9, 2023

Accepted: March 7, 2023

Published: March 29, 2023

Web resources

ClinVar, <https://www.ncbi.nlm.nih.gov/clinvar/>

OMIM, <https://www.omim.org/>

References

1. Olusanya, B.O., Wright, S.M., Nair, M.K.C., Boo, N.Y., Halpern, R., Kuper, H., Abubakar, A.A., Almasri, N.A., Arabloo, J., Arora, N.K., et al. (2020). Global burden of childhood epilepsy, intellectual disability, and sensory impairments. *Pediatrics* 146, e20192623. <https://doi.org/10.1542/peds.2019-2623>.
2. Parenti, I., Rabaneda, L.G., Schoen, H., and Novarino, G. (2020). Neurodevelopmental disorders: from genetics to functional pathways. *Trends Neurosci.* 43, 608–621. <https://doi.org/10.1016/j.tins.2020.05.004>.
3. Engbers, H.M., Nievelstein, R.A.J., Gooskens, R.H.J.M., Kroes, H.Y., van Empelen, R., Braams, O., Wittebol-Post, D., Hendriks, M.M.W.B., and Visser, G. (2010). The clinical utility of MRI in patients with neurodevelopmental disorders of unknown origin. *Eur. J. Neurol.* 17, 815–822. <https://doi.org/10.1111/j.1468-1331.2009.02927.x>.
4. Retterer, K., Juusola, J., Cho, M.T., Vitazka, P., Millan, F., Gibellini, F., Vertino-Bell, A., Smaoui, N., Neidich, J., Monaghan, K.G., et al. (2016). Clinical application of whole-exome sequencing across clinical indications. *Genet. Med.* 18, 696–704. <https://doi.org/10.1038/gim.2015.148>.
5. Mitani, T., Isikay, S., Gezdirici, A., Gulec, E.Y., Punetha, J., Fatih, J.M., Herman, I., Akay, G., Du, H., Calame, D.G., et al. (2021). High prevalence of multilocus pathogenic variation in neurodevelopmental disorders in the Turkish population. *Am. J. Hum. Genet.* 108, 1981–2005. <https://doi.org/10.1016/j.ajhg.2021.08.009>.
6. Srivastava, S., Love-Nichols, J.A., Dies, K.A., Ledbetter, D.H., Martin, C.L., Chung, W.K., Firth, H.V., Frazier, T., Hansen, R.L., Prock, L., et al. (2019). Meta-analysis and multidisciplinary consensus statement: exome sequencing is a first-tier clinical diagnostic test for individuals with neurodevelopmental disorders. *Genet. Med.* 21, 2413–2421. <https://doi.org/10.1038/s41436-019-0554-6>.
7. Thevenon, J., Duffourd, Y., Masurel-Paulet, A., Lefebvre, M., Feillet, F., El Chehadeh-Djebbar, S., St-Onge, J., Steinmetz, A., Huet, F., Chouchane, M., et al. (2016). Diagnostic odyssey in severe neurodevelopmental disorders: toward clinical whole-exome sequencing as a first-line diagnostic test. *Clin. Genet.* 89, 700–707. <https://doi.org/10.1111/cge.12732>.
8. Vrijenhoek, T., Middelburg, E.M., Monroe, G.R., van Gassen, K.L.I., Geenen, J.W., Hövels, A.M., Knoers, N.V., van Amstel, H.K.P., and Frederix, G.W.J. (2018). Whole-exome sequencing in intellectual disability; cost before and after a diagnosis. *Eur. J. Hum. Genet.* 26, 1566–1571. <https://doi.org/10.1038/s41431-018-0203-6>.
9. Geisheker, M.R., Heymann, G., Wang, T., Coe, B.P., Turner, T.N., Stessman, H.A.F., Hoekzema, K., Kvarnung, M., Shaw, M., Friend, K., et al. (2017). Hotspots of missense mutation identify neurodevelopmental disorder genes and functional domains. *Nat. Neurosci.* 20, 1043–1051. <https://doi.org/10.1038/nn.4589>.
10. Lindstrand, A., Eisfeldt, J., Pettersson, M., Carvalho, C.M.B., Kvarnung, M., Grigelioniene, G., Anderlid, B.M., Bjerin, O., Gustavsson, P., Hammarsjö, A., et al. (2019). From cytogenetics to cytogenomics: whole-genome sequencing as a

- first-line test comprehensively captures the diverse spectrum of disease-causing genetic variation underlying intellectual disability. *Genome Med.* 11, 68. <https://doi.org/10.1186/s13073-019-0675-1>.
11. Martinez-Granero, F., Blanco-Kelly, F., Sanchez-Jimeno, C., Avila-Fernandez, A., Arceche, A., Bustamante-Aragones, A., Rodilla, C., Rodríguez-Pinilla, E., Riveiro-Alvarez, R., Tahsin-Swafiri, S., et al. (2021). Comparison of the diagnostic yield of aCGH and genome-wide sequencing across different neurodevelopmental disorders. *NPJ Genom. Med.* 6, 25. <https://doi.org/10.1038/s41525-021-00188-7>.
 12. Hiz Kurul, S., Oktay, Y., Töpf, A., Szabó, N.Z., Güngör, S., Yaramis, A., Sonmezler, E., Matalonga, L., Yis, U., Schon, K., et al. (2022). High diagnostic rate of trio exome sequencing in consanguineous families with neurogenetic diseases. *Brain* 145, 1507–1518. <https://doi.org/10.1093/brain/awab395>.
 13. Dingemans, A.J.M., Hinne, M., Jansen, S., van Reeuijck, J., de Leeuw, N., Pfundt, R., van Bon, B.W., Vulto-van Silfhout, A.T., Kleefstra, T., Koolen, D.A., et al. (2022). Phenotype based prediction of exome sequencing outcome using machine learning for neurodevelopmental disorders. *Genet. Med.* 24, 645–653. <https://doi.org/10.1016/j.gim.2021.10.019>.
 14. Vohr, B., Allan, W.C., Scott, D.T., Katz, K.H., Schneider, K.C., Makuch, R.W., and Ment, L.R. (1999). Early-onset intraventricular hemorrhage in preterm neonates: incidence of neurodevelopmental handicap. *Semin. Perinatol.* 23, 212–217. [https://doi.org/10.1016/s0146-0005\(99\)80065-2](https://doi.org/10.1016/s0146-0005(99)80065-2).
 15. Moretti, R., Pansiot, J., Bettati, D., Strazielle, N., Ghersi-Egea, J.F., Damante, G., Fleiss, B., Titomanlio, L., and Gressens, P. (2015). Blood-brain barrier dysfunction in disorders of the developing brain. *Front. Neurosci.* 9, 40. <https://doi.org/10.3389/fnins.2015.00040>.
 16. De Haan, T.R., Langeslag, J., van der Lee, J.H., and van Kaam, A.H. (2018). A systematic review comparing neurodevelopmental outcome in term infants with hypoxic and vascular brain injury with and without seizures. *BMC Pediatr.* 18, 147. <https://doi.org/10.1186/s12887-018-1116-9>.
 17. Gilard, V., Chadie, A., Ferracci, F.X., Brasseur-Daudruy, M., Proust, F., Marret, S., and Curey, S. (2018). Post hemorrhagic hydrocephalus and neurodevelopmental outcomes in a context of neonatal intraventricular hemorrhage: an institutional experience in 122 preterm children. *BMC Pediatr.* 18, 288. <https://doi.org/10.1186/s12887-018-1249-x>.
 18. Sileo, F.G., Zöllner, J., D'Antonio, F., Islam, S., Papageorgiou, A.T., and Khalil, A. (2022). Perinatal and long-term outcome of fetal intracranial hemorrhage: systematic review and meta-analysis. *Ultrasound Obstet. Gynecol.* 59, 585–595. <https://doi.org/10.1002/uog.24766>.
 19. Cen, Z., Chen, Y., Chen, S., Wang, H., Yang, D., Zhang, H., Wu, H., Wang, L., Tang, S., Ye, J., et al. (2020). Biallelic loss-of-function mutations in *JAM2* cause primary familial brain calcification. *Brain* 143, 491–502. <https://doi.org/10.1093/brain/awz392>.
 20. Schottlaender, L.V., Abeti, R., Jaunmuktane, Z., Macmillan, C., Chelban, V., O'Callaghan, B., McKinley, J., Maroofian, R., Efthymiou, S., Athanasiou-Fragkouli, A., et al. (2020). Biallelic *JAM2* variants lead to early-onset recessive primary familial brain calcification. *Am. J. Hum. Genet.* 106, 412–421. <https://doi.org/10.1016/j.ajhg.2020.02.007>.
 21. Mochida, G.H., Ganesh, V.S., Felie, J.M., Gleason, D., Hill, R.S., Clapham, K.R., Rakiec, D., Tan, W.H., Akawi, N., Al-Saffar, M., et al. (2010). A homozygous mutation in the tight-junction protein *JAM3* causes hemorrhagic destruction of the brain, subependymal calcification, and congenital cataracts. *Am. J. Hum. Genet.* 87, 882–889. <https://doi.org/10.1016/j.ajhg.2010.10.026>.
 22. Akawi, N.A., Canpolat, F.E., White, S.M., Quilis-Esquerria, J., Morales Sanchez, M., Gamundi, M.J., Mochida, G.H., Walsh, C.A., Ali, B.R., and Al-Gazali, L. (2013). Delineation of the clinical, molecular and cellular aspects of novel *JAM3* mutations underlying the autosomal recessive hemorrhagic destruction of the brain, subependymal calcification, and congenital cataracts. *Hum. Mutat.* 34, 498–505. <https://doi.org/10.1002/humu.22263>.
 23. O'Driscoll, M.C., Daly, S.B., Urquhart, J.E., Black, G.C.M., Pilz, D.T., Brockmann, K., McEntagart, M., Abdel-Salam, G., Zaki, M., Wolf, N.I., et al. (2010). Recessive mutations in the gene encoding the tight junction protein occludin cause band-like calcification with simplified gyration and polymicrogyria. *Am. J. Hum. Genet.* 87, 354–364. <https://doi.org/10.1016/j.ajhg.2010.07.012>.
 24. Abdel-Hamid, M.S., Abdel-Salam, G.M.H., Issa, M.Y., Emam, B.A., and Zaki, M.S. (2017). Band-like calcification with simplified gyration and polymicrogyria: report of 10 new families and identification of five novel *OCLN* mutations. *J. Hum. Genet.* 62, 553–559. <https://doi.org/10.1038/jhg.2017.4>.
 25. Sobreira, N., Schiettecatte, F., Valle, D., and Hamosh, A. (2015). GeneMatcher: a matching tool for connecting investigators with an interest in the same gene. *Hum. Mutat.* 36, 928–930. <https://doi.org/10.1002/humu.22844>.
 26. Jin, S.C., Dong, W., Kundishora, A.J., Panchagnula, S., Moreno-De-Luca, A., Furey, C.G., Allocco, A.A., Walker, R.L., Nelson-Williams, C., Smith, H., et al. (2020). Exome sequencing implicates genetic disruption of prenatal neurogenesis in sporadic congenital hydrocephalus. *Nat. Med.* 26, 1754–1765. <https://doi.org/10.1038/s41591-020-1090-2>.
 27. Saudi Mendeliome Group (2015). Comprehensive gene panels provide advantages over clinical exome sequencing for Mendelian diseases. *Genome Biol.* 16, 134. <https://doi.org/10.1186/s13059-015-0693-2>.
 28. Abouelhoda, M., Sobahy, T., El-Kalioby, M., Patel, N., Shamseldin, H., Monies, D., Al-Tassan, N., Ramzan, K., Imtiaz, F., Shaheen, R., and Alkuraya, F.S. (2016). Clinical genomics can facilitate countrywide estimation of autosomal recessive disease burden. *Genet. Med.* 18, 1244–1249. <https://doi.org/10.1038/gim.2016.37>.
 29. Fattahi, Z., Beheshtian, M., Mohseni, M., Poustchi, H., Sellars, E., Nezhadi, S.H., Amini, A., Arzhang, S., Jalalvand, K., Jamali, P., et al. (2019). Iranome: A catalog of genomic variations in the Iranian population. *Hum. Mutat.* 40, 1968–1984. <https://doi.org/10.1002/humu.23880>.
 30. Scott, E.M., Halees, A., Itan, Y., Spencer, E.G., He, Y., Azab, M.A., Gabriel, S.B., Belkadi, A., Boisson, B., Abel, L., et al. (2016). Characterization of Greater Middle Eastern genetic variation for enhanced disease gene discovery. *Nat. Genet.* 48, 1071–1076. <https://doi.org/10.1038/ng.3592>.
 31. Kars, M.E., Başak, A.N., Onat, O.E., Bilguvar, K., Choi, J., Itan, Y., Çağlar, C., Palvadeau, R., Casanova, J.L., Cooper, D.N., et al. (2021). The genetic structure of the Turkish population reveals high levels of variation and admixture. *Proc. Natl. Acad. Sci. USA* 118. e2026076118. <https://doi.org/10.1073/pnas.2026076118>.
 32. Ishida, T., Kundu, R.K., Yang, E., Hirata, K.i., Ho, Y.D., and Quertermous, T. (2003). Targeted disruption of endothelial

- cell-selective adhesion molecule inhibits angiogenic processes in vitro and in vivo. *J. Biol. Chem.* 278, 34598–34604. <https://doi.org/10.1074/jbc.M304890200>.
33. Wegmann, F., Petri, B., Khandoga, A.G., Moser, C., Khandoga, A., Volkery, S., Li, H., Nasdala, I., Brandau, O., Fässler, R., et al. (2006). ESAM supports neutrophil extravasation, activation of Rho, and VEGF-induced vascular permeability. *J. Exp. Med.* 203, 1671–1677. <https://doi.org/10.1084/jem.20060565>.
 34. Hirata, K.I., Ishida, T., Penta, K., Rezaee, M., Yang, E., Wohlge-muth, J., and Quertermous, T. (2001). Cloning of an immuno-globulin family adhesion molecule selectively expressed by endothelial cells. *J. Biol. Chem.* 276, 16223–16231. <https://doi.org/10.1074/jbc.M100630200>.
 35. Nasdala, I., Wolburg-Buchholz, K., Wolburg, H., Kuhn, A., Eb-net, K., Brachtendorf, G., Samulowitz, U., Kuster, B., Engelhardt, B., Vestweber, D., and Butz, S. (2002). A transmembrane tight junction protein selectively expressed on endothelial cells and platelets. *J. Biol. Chem.* 277, 16294–16303. <https://doi.org/10.1074/jbc.M111999200>.
 36. Hara, T., Ishida, T., Cangara, H.M., and Hirata, K.I. (2009). Endothelial cell-selective adhesion molecule regulates albuminuria in diabetic nephropathy. *Microvasc. Res.* 77, 348–355. <https://doi.org/10.1016/j.mvr.2009.01.002>.
 37. Kobayashi, H., Looker, H.C., Satake, E., Saulnier, P.J., Md Dom, Z.I., O'Neil, K., Ihara, K., Krolewski, B., Galecki, A.T., Niewczas, M.A., et al. (2022). Results of untargeted analysis using the SOMAscan proteomics platform indicates novel associations of circulating proteins with risk of progression to kidney failure in diabetes. *Kidney Int.* 102, 370–381. <https://doi.org/10.1016/j.kint.2022.04.022>.
 38. Gallardo-Vara, E., Ruiz-Llorente, L., Casado-Vela, J., Ruiz-Rodríguez, M.J., López-Andrés, N., Pattnaik, A.K., Quintanilla, M., and Bernabeu, C. (2019). Endoglin Protein Interac-tome Profiling Identifies TRIM21 and Galectin-3 as New Binding Partners. *Cells* 8, 1082. <https://doi.org/10.3390/cells8091082>.
 39. Xu, B., Roos, J.L., Dexheimer, P., Boone, B., Plummer, B., Levy, S., Gogos, J.A., and Karayiorgou, M. (2011). Exome sequencing supports a de novo mutational paradigm for schizophrenia. *Nat. Genet.* 43, 864–868. <https://doi.org/10.1038/ng.902>.
 40. Collins, R.L., Glessner, J.T., Porcu, E., Lepamets, M., Brandon, R., Lauricella, C., Han, L., Morley, T., Niestroj, L.M., Ulirsch, J., et al. (2022). A cross-disorder dosage sensitivity map of the human genome. *Cell* 185, 3041–3055.e25. <https://doi.org/10.1016/j.cell.2022.06.036>.
 41. de Vries, L.S., Koopman, C., Groenendaal, F., Van Schooneveld, M., Verheijen, F.W., Verbeek, E., Witkamp, T.D., van der Worp, H.B., and Mancini, G. (2009). *COL4A1* mutation in two preterm siblings with antenatal onset of parenchymal hemorrhage. *Ann. Neurol.* 65, 12–18. <https://doi.org/10.1002/ana.21525>.
 42. Yoneda, Y., Haginoya, K., Kato, M., Osaka, H., Yokochi, K., Arai, H., Kakita, A., Yamamoto, T., Otsuki, Y., Shimizu, S.i., et al. (2013). Phenotypic spectrum of *COL4A1* mutations: por-encephaly to schizencephaly. *Ann. Neurol.* 73, 48–57. <https://doi.org/10.1002/ana.23736>.
 43. Meuwissen, M.E.C., Halley, D.J.J., Smit, L.S., Lequin, M.H., Cobben, J.M., de Coo, R., van Harsseel, J., Sallevelt, S., Wol-dringh, G., van der Knaap, M.S., et al. (2015). The expanding phenotype of *COL4A1* and *COL4A2* mutations: clinical data on 13 newly identified families and a review of the liter-ature. *Genet. Med.* 17, 843–853. <https://doi.org/10.1038/gim.2014.210>.
 44. Alavi, M.V., Mao, M., Pawlikowski, B.T., Kvezereli, M., Dun-can, J.L., Libby, R.T., John, S.W.M., and Gould, D.B. (2016). *Col4a1* mutations cause progressive retinal neovascular de-fects and retinopathy. *Sci. Rep.* 6, 18602. <https://doi.org/10.1038/srep18602>.
 45. Zagaglia, S., Selch, C., Nisevic, J.R., Mei, D., Michalak, Z., Her-nandez-Hernandez, L., Krithika, S., Vezyroglou, K., Varadkar, S.M., Pepler, A., et al. (2018). Neurologic phenotypes associ-ated with *COL4A1/2* mutations: Expanding the spectrum of disease. *Neurology* 91, e2078–e2088. <https://doi.org/10.1212/WNL.0000000000006567>.
 46. Srivastava, S., Lewis, S.A., Cohen, J.S., Zhang, B., Aravamuthan, B.R., Chopra, M., Sahin, M., Kruer, M.C., and Po-duri, A. (2022). Molecular diagnostic yield of exome sequencing and chromosomal microarray in cerebral palsy: a systematic review and meta-analysis. *JAMA Neurol.* 79, 1287–1295. <https://doi.org/10.1001/jamaneurol.2022.3549>.
 47. Lacoste, B., Comin, C.H., Ben-Zvi, A., Kaeser, P.S., Xu, X., Costa, L.d.F., and Gu, C. (2014). Sensory-related neural activ-ity regulates the structure of vascular networks in the cerebral cortex. *Neuron* 83, 1117–1130. <https://doi.org/10.1016/j.neuron.2014.07.034>.
 48. Andreone, B.J., Lacoste, B., and Gu, C. (2015). Neuronal and vascular interactions. *Annu. Rev. Neurosci.* 38, 25–46. <https://doi.org/10.1146/annurev-neuro-071714-033835>.
 49. Kugler, E.C., Greenwood, J., and MacDonald, R.B. (2021). The "neuro-glia-vascular" unit: the role of glia in neurovascular unit formation and dysfunction. *Front. Cell Dev. Biol.* 9, 732820. <https://doi.org/10.3389/fcell.2021.732820>.
 50. Zisis, E., Keller, D., Kanari, L., Arnaudon, A., Gevaert, M., Del-emontex, T., Coste, B., Foni, A., Abdallah, M., Cali, C., et al. (2021). Digital reconstruction of the neuro-glia-vascular archi-tecture. *Cereb. Cortex* 31, 5686–5703. <https://doi.org/10.1093/cercor/bhab254>.
 51. Ouellette, J., Toussay, X., Comin, C.H., Costa, L.D.F., Ho, M., Lacalle-Auriales, M., Freitas-Andrade, M., Liu, Q.Y., Leclerc, S., Pan, Y., et al. (2020). Vascular contributions to 16p11.2 deletion autism syndrome modeled in mice. *Nat. Neurosci.* 23, 1090–1101. <https://doi.org/10.1038/s41593-020-0663-1>.
 52. Azmitia, E.C., Saccomano, Z.T., Alzoobae, M.F., Boldrini, M., and Whitaker-Azmitia, P.M. (2016). Persistent angiogenesis in the autism brain: an immunocytochemical study of postmor-tem cortex, brainstem and cerebellum. *J. Autism Dev. Disord.* 46, 1307–1318. <https://doi.org/10.1007/s10803-015-2672-6>.
 53. Jann, K., Hernandez, L.M., Beck-Pancer, D., McCarron, R., Smith, R.X., Dapretto, M., and Wang, D.J.J. (2015). Altered resting perfusion and functional connectivity of default mode network in youth with autism spectrum disorder. *Brain Behav.* 5, e00358. <https://doi.org/10.1002/brb3.358>.